

Lattice 2007, Regensburg

Extreme QCD 2007, Frascati

Phase-Quenched Lattice QCD at Finite Density and Temperature

D. K. Sinclair and J. B. Kogut

- Introduction
- Phase-Quenched Lattice QCD
- Simulations and Results
- Equation-of-State
- Discussion and conclusions

Introduction

Simulation methods, based on importance sampling, fail for QCD at finite quark-/baryon-number density. If we use a quark-number chemical potential μ to produce finite density, the fermion determinant becomes complex. If we use canonical ensemble methods, the projection on to states of definite quark number gives rise to a sign problem.

Some progress has been made in circumventing these problems for small μ , close to the finite-temperature transition, the region of relevance to heavy-ion colliders, where the sign problems appear to be under control. These methods include methods which exploit the analyticity in μ near $\mu = 0$, reweighting methods, canonical ensemble methods and phase quenching. In this part of the phase diagram, the most interesting feature is expected to be the critical endpoint where the finite-temperature

transition changes from a crossover to a first-order phase transition at an Ising critical point.

We are performing simulations of phase-quenched lattice QCD, i.e. lattice QCD where the fermion determinant is replaced by its magnitude, at finite $\mu_I = 2\mu$. For $\mu < m_\pi/2$ it is expected that this theory will have the same phase structure as full QCD. We are simulating 3-flavour QCD close to the critical mass (at $\mu = 0$), where it was hoped that this critical point might morph into the critical endpoint.

We are extending our simulations to examine the equation-of-state (EOS) of phase-quenched QCD.

$N_f=3$ lattice QCD

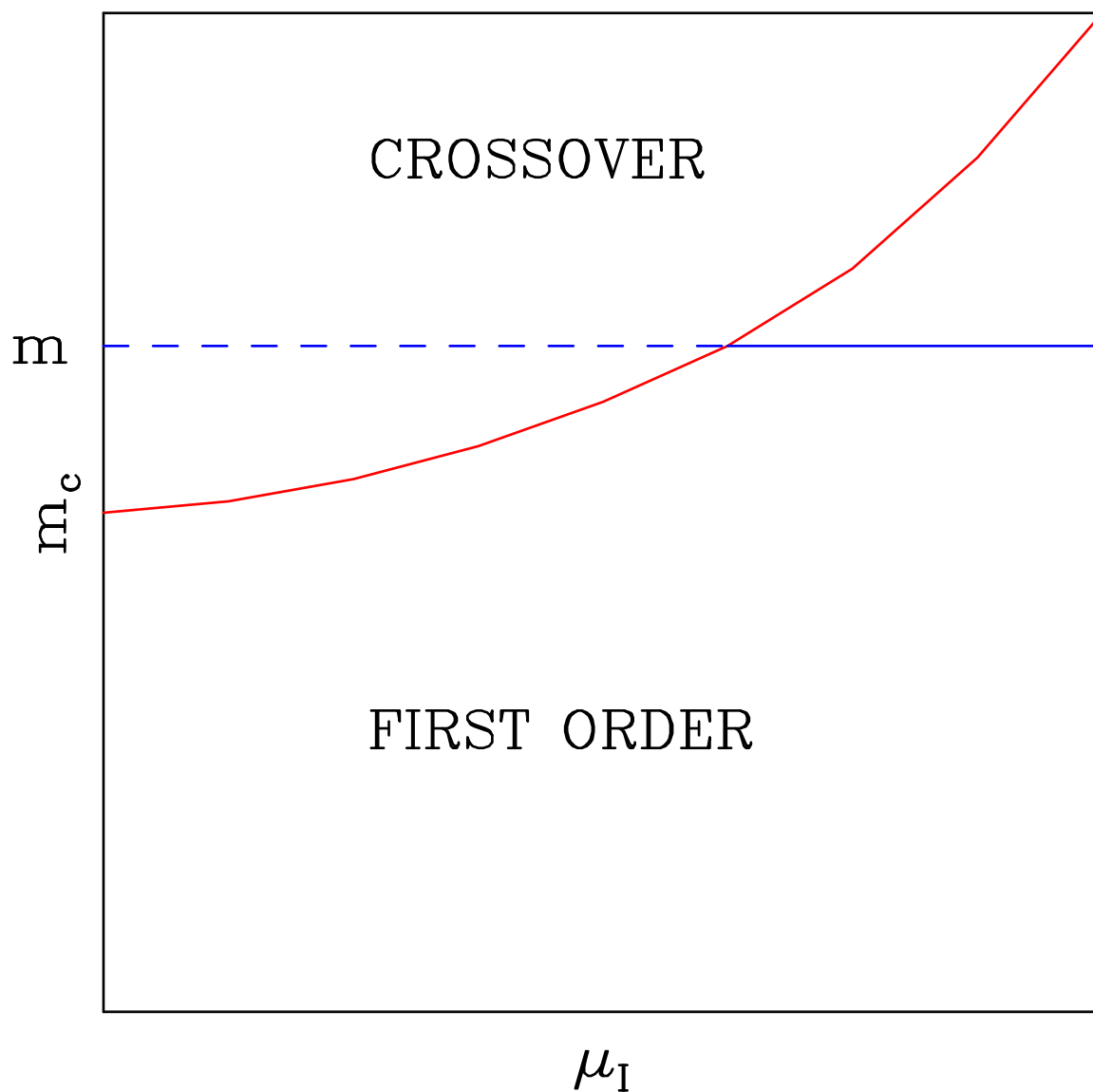


Figure 1: Nature of finite temperature phase transition if m_c increases with $\mu(\mu_I)$.

Phase-Quenched Lattice QCD

The staggered quark action for lattice QCD with N_f quark flavours at finite chemical potential μ , expressed in terms of the pseudo-fermion field χ is:

$$S_{pf} = \chi^\dagger M^{-N_f/4} \chi$$

where

$$M = \mathcal{D}(\mu) + m$$

and $\mathcal{D}(\mu)$ is the standard staggered-quark \mathcal{D} with the links in the $+t$ direction multiplied by e^μ and those in the $-t$ direction multiplied by $e^{-\mu}$.

The phase-quenched action is:

$$S_{pf} = \chi^\dagger \mathcal{M}^{-N_f/8} \chi$$

where

$$\mathcal{M} = M^\dagger M$$

which is positive (semi-)definite. For $\mu < m_\pi/2$ its spectrum is expected to have a positive lower

bound, except possibly on a set of configurations of measure zero. It is useful to define

$$\mu_I = 2\mu$$

which has the interpretation of an isospin (I_3) chemical potential (at least for N_f even).

We now use the exact RHMC algorithm for our simulations, using a speculative lower bound for the spectrum of the Dirac operator.

At zero temperature, the effect of a small μ_I is to lower the effective mass of one of the pions to

$$m_{eff} = m_\pi - \mu_I.$$

Thus this pion becomes a massless Goldstone boson at $\mu_I = m_\pi$, and there is a phase transition to a superfluid phase at this point. This superfluid phase persists to finite temperature, and its boundary gives a natural limit to the validity of the phase-quenched approximation. The large fluctuations of the phase of the fermion determinant at

this boundary are expected to suppress this phase transition for full QCD. Such fluctuations have been seen in random-matrix models which mimic QCD.

Simulations and Results

We simulate 3-flavour QCD at small ‘isospin’ (I_3) chemical potential μ_I , on $8^3 \times 4$, $12^3 \times 4$ and $16^3 \times 4$ lattices, in the neighbourhood of the finite temperature transition. Since $m_c(\mu_I = 0) = 0.0265(3)$ (measured in these simulations), we run with quark mass $m = 0.020, 0.025, 0.030, 0.035$. We run at $\mu_I = 0.0, 0.2, 0.3$ ($\mu_I < m_\pi$). Since high statistics are needed we perform runs of 300,000 trajectories for each of 4 β values close to the transition for each (m, μ_I) on the $12^3 \times 4$ lattice.

To determine the nature of the transition, we measure the 4th-order Binder cumulant (B_4) for the chiral condensate. For any observable X ,

$$B_4(X) = \frac{\langle (X - \langle X \rangle)^4 \rangle}{\langle (X - \langle X \rangle)^2 \rangle^2}. \quad (1)$$

Since we only have stochastic estimators for $\langle \bar{\psi}\psi \rangle$,

we need at least 4 independent estimators for each configuration – we use 5.

If there is a critical endpoint at small μ_I for $m > m_c(0)$, then the Binder cumulant should decrease from its crossover value $B_4 = 3$ passing through the Ising value $B_4 = 1.604(1)$ at the endpoint, and falling towards its first-order value $B_4 = 1$ as μ_I is increased. The ‘data’ for $m = 0.035$ and $m = 0.030$ do not show this. In fact, B_4 appears to increase with increasing μ_I . At fixed *physical* quark mass, this increase would be even more pronounced.

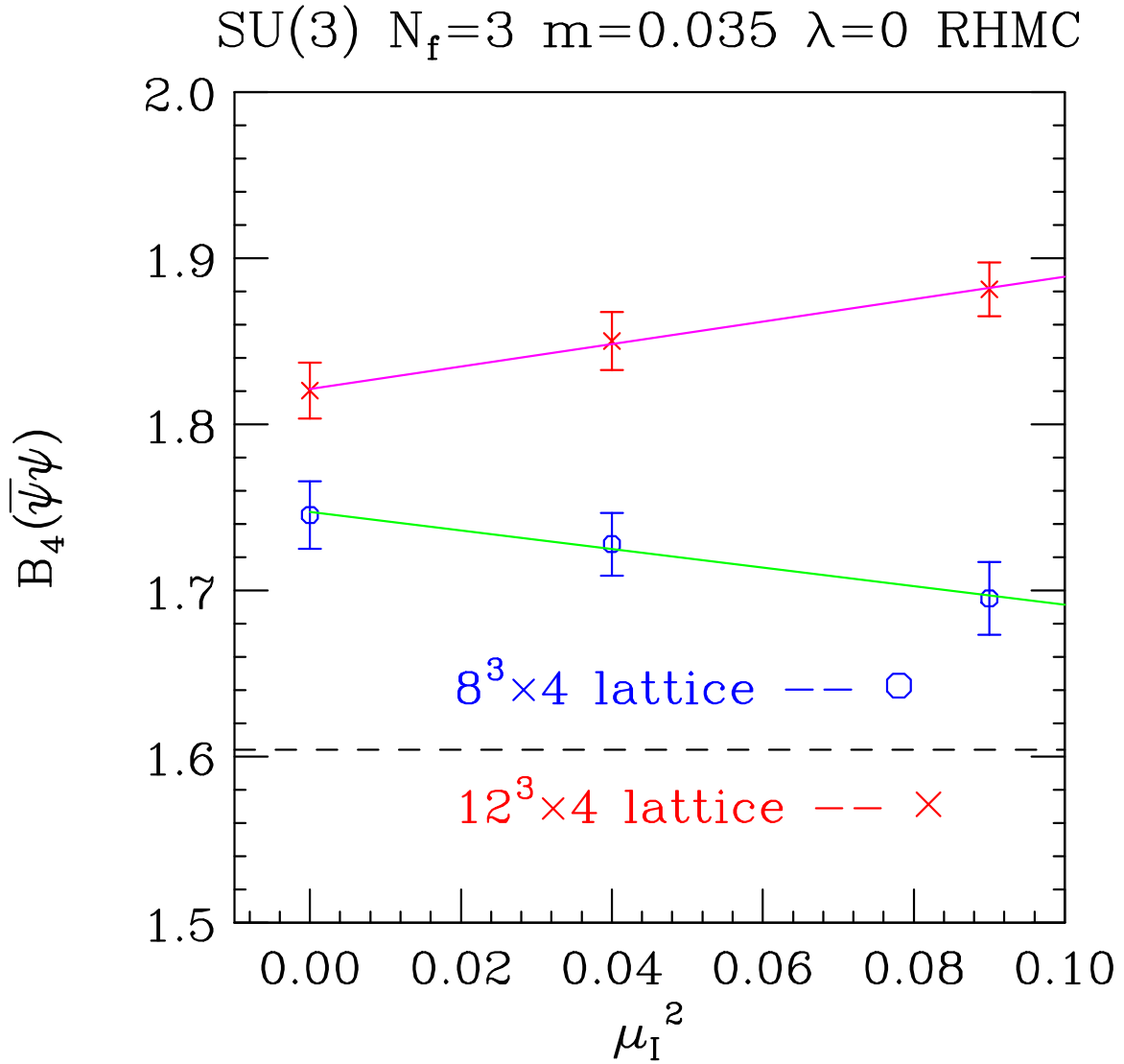


Figure 2: Binder cumulant at $T = T_c$ as a function of μ_I^2 at $m = 0.035$.

SU(3) $N_f=3$ $m=0.03$ $\lambda=0$ RHMC

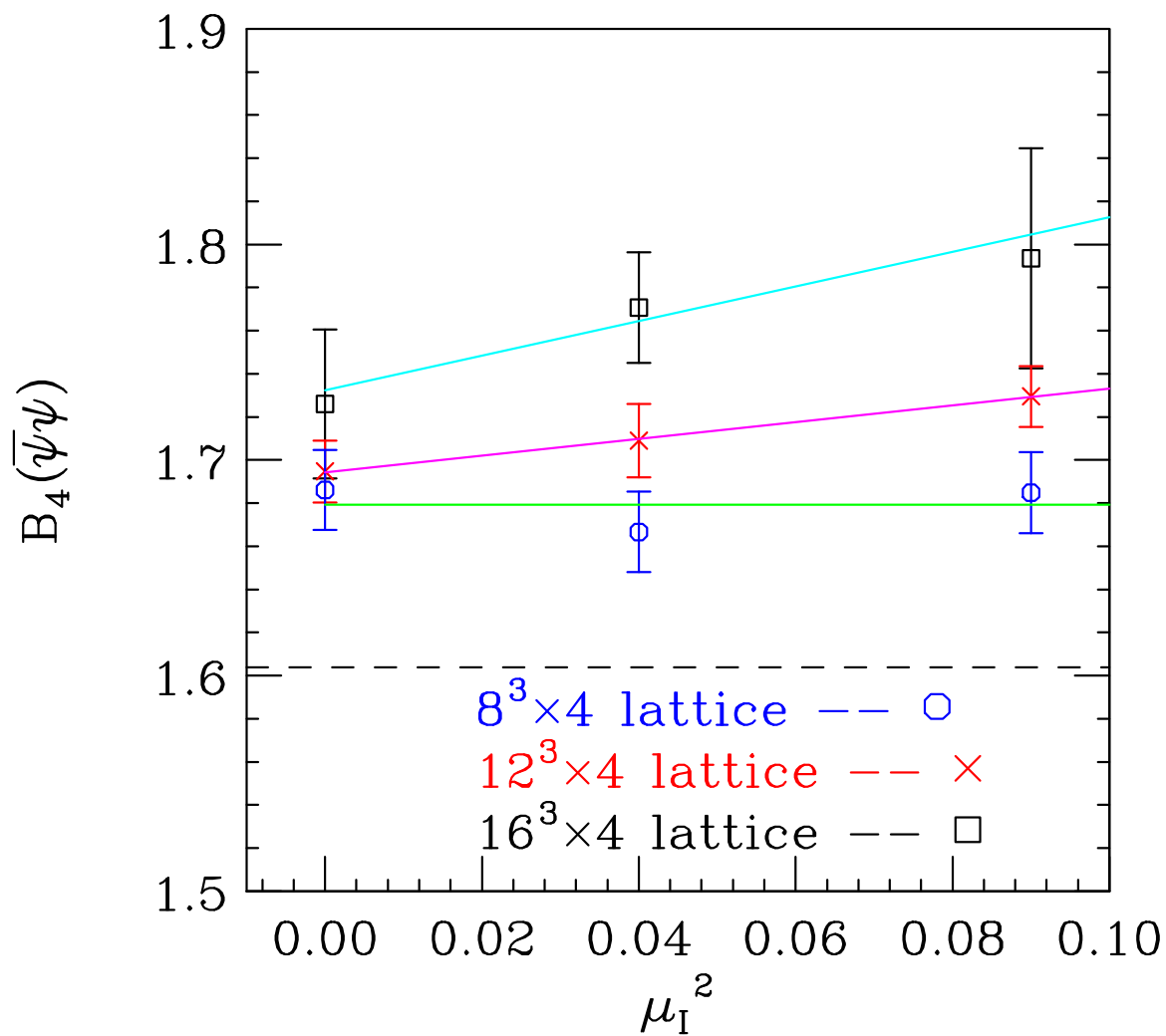


Figure 3: Binder cumulant at $T = T_c$ as a function of μ_I^2 at $m = 0.030$.

SU(3) $N_f=3$ $m=0.025$ $\lambda=0$ RHMC

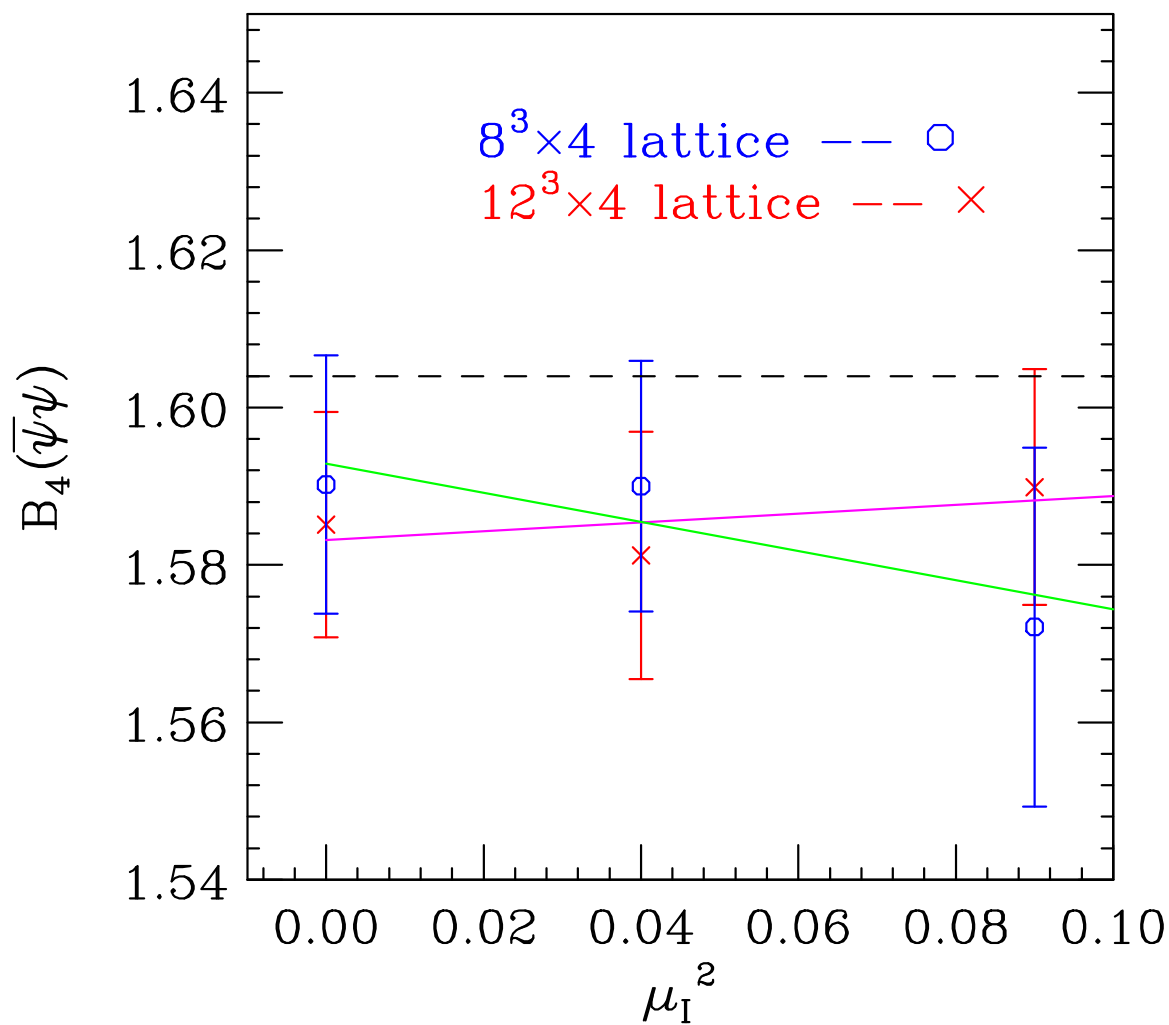


Figure 4: Binder cumulant at $T = T_c$ as a function of μ_I^2 at $m = 0.025$.

The chiral condensate is not the order parameter (magnetization), since $m \neq 0$. For $\mu_I = 0$, the order parameter, a renormalization group scaling operator will have the form

$$\mathcal{M} = \bar{\psi}\psi + yS_g$$

where

$$S_g = 1 - \frac{1}{3}\text{Re}[\text{Tr}(UUUU)].$$

For $\mu_I \neq 0$, it will have the form

$$\mathcal{M} = \bar{\psi}\psi + xj_0^3 + yS_g$$

where j_0^3 is the isospin (I_3) density.

On large lattices, which we use makes no difference, but on finite lattices the correct choice of \mathcal{M} will show the smallest finite volume corrections. One indication of how much error is incurred by using $\bar{\psi}\psi$ instead of \mathcal{M} is how close the intersection of the graphs of Binder cumulants is to the Ising

value. The plots of $B_4(\bar{\psi}\psi)$ at fixed μ_I indicate that choosing $x = y = 0$ is probably adequate.

μ_I	$m_c(\mu_I)$
0.0	0.0265(3)
0.2	0.0259(5)
0.3	0.0256(4)

$m_c(\mu_I)$, in lattice units, is almost independent of μ_I . Since β_c and hence T_c decrease with increasing μ_I , $m_c(\mu_I)$, in physical units, decreases with increasing μ_I and so does not yield a critical endpoint.

SU(3) $N_f=3$ $\mu_I=0$ $\lambda=0$

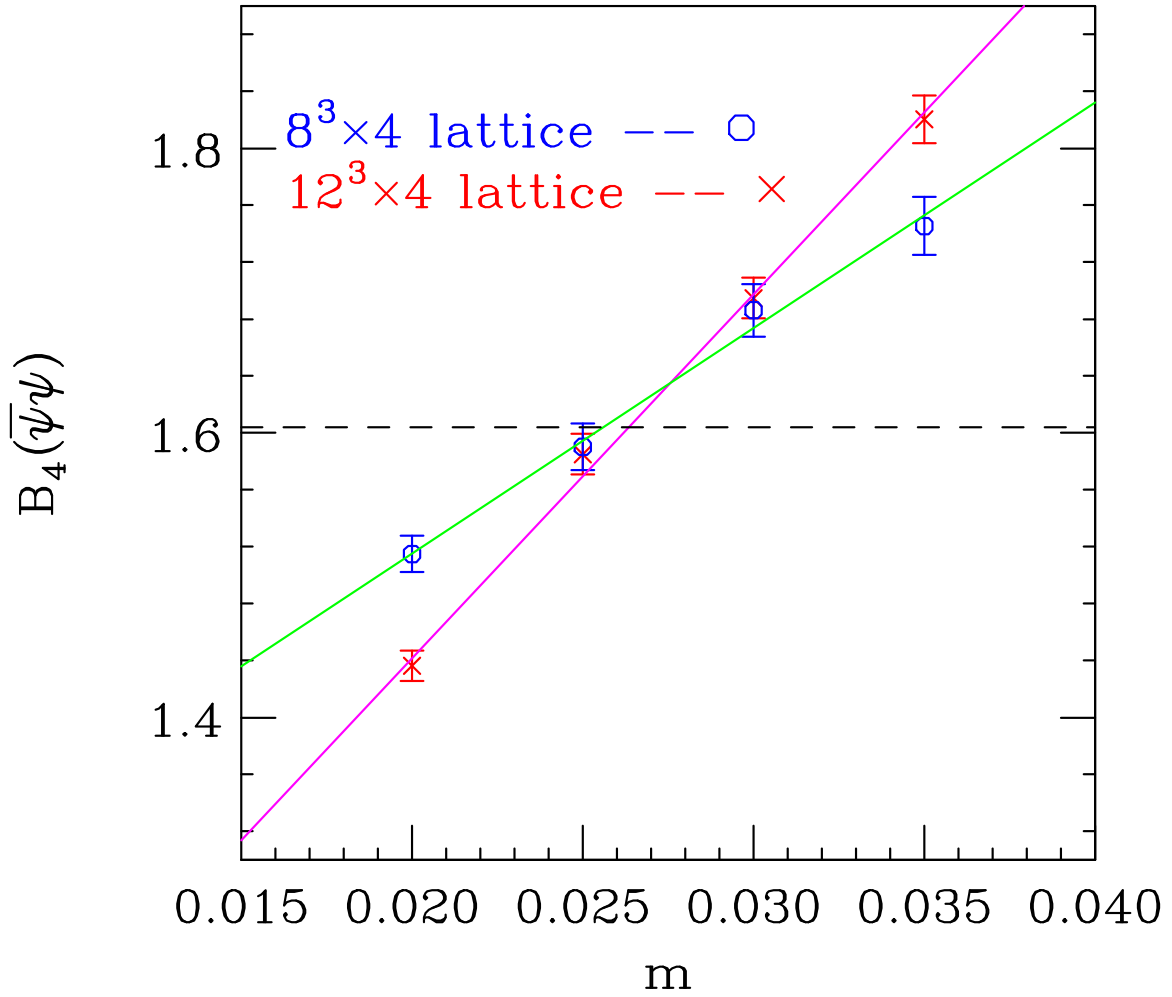


Figure 5: $B_4(\bar{\psi}\psi)$ at $\mu_I = 0$ as functions of mass.

SU(3) $N_f=3$ $\mu_I=0.2$ $\lambda=0$

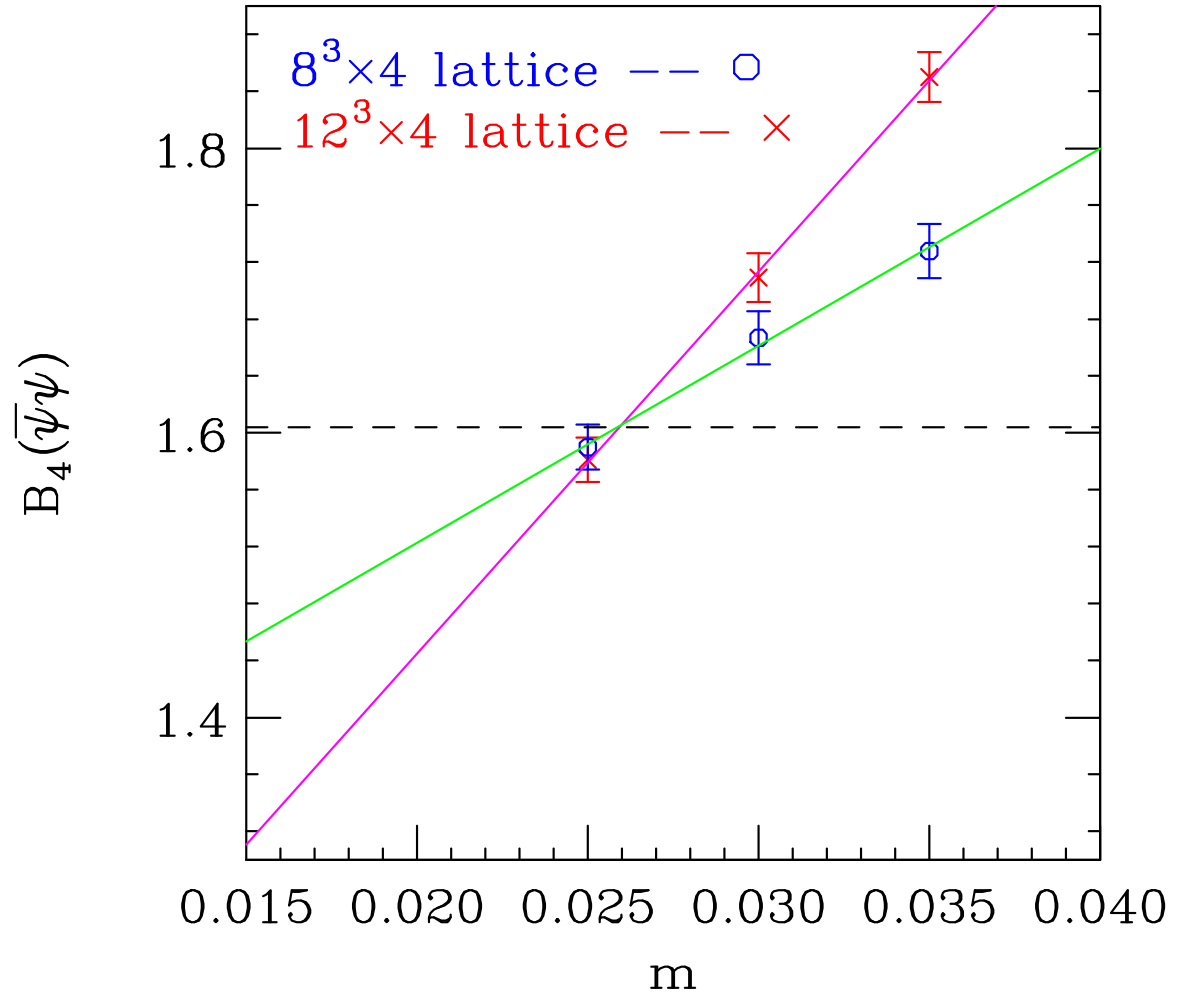


Figure 6: $B_4(\bar{\psi}\psi)$ at $\mu_I = 0.2$ as functions of mass.

SU(3) $N_f=3$ $\mu_I=0.3$ $\lambda=0$

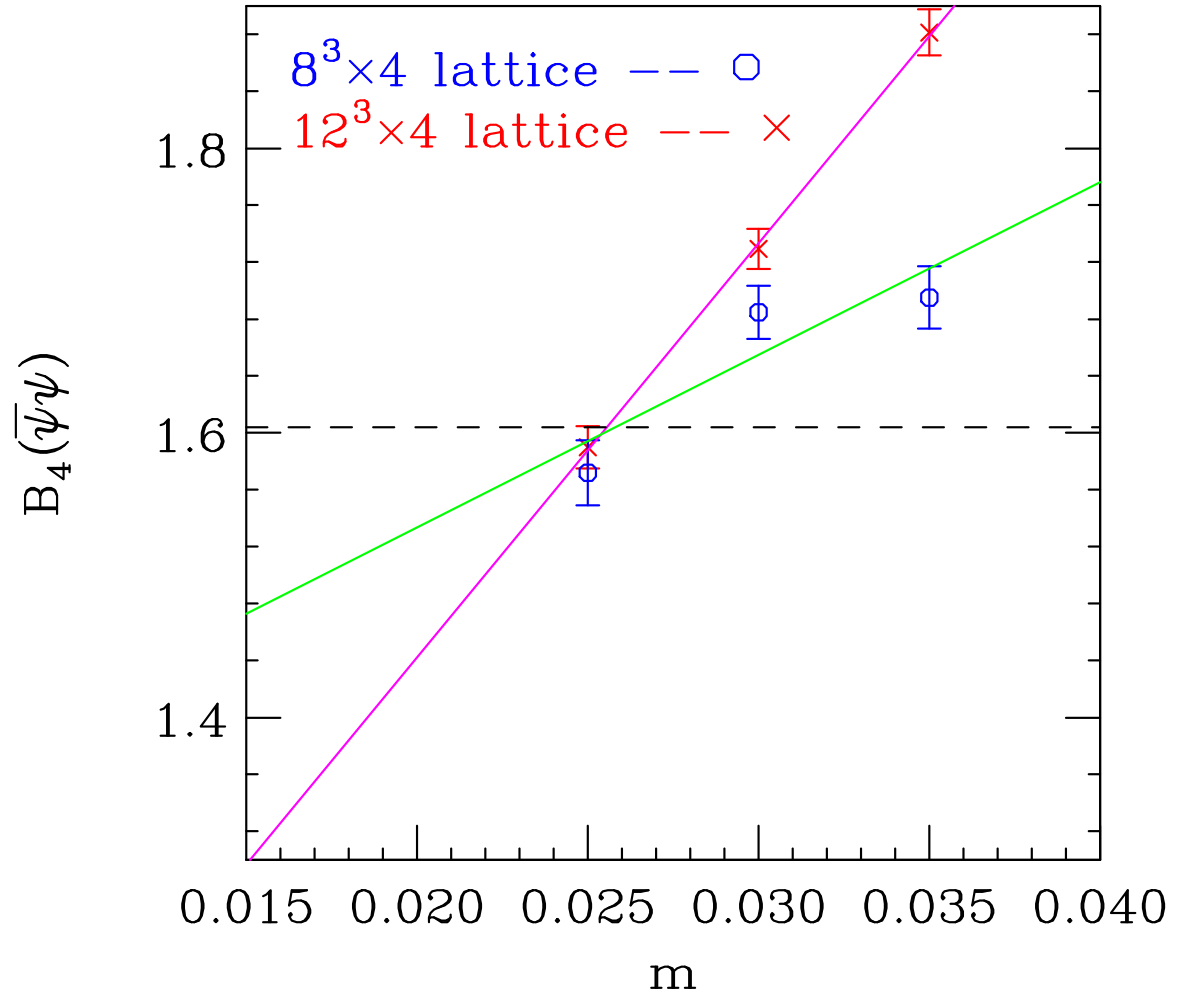


Figure 7: $B_4(\bar{\psi}\psi)$ at $\mu_I = 0.3$ as functions of mass.

If our original fields ($\bar{\psi}\psi$, S_g and j_0^3) were the true scaling fields, fluctuations of these quantities would be independent. The graphs which follow show that this is not so.

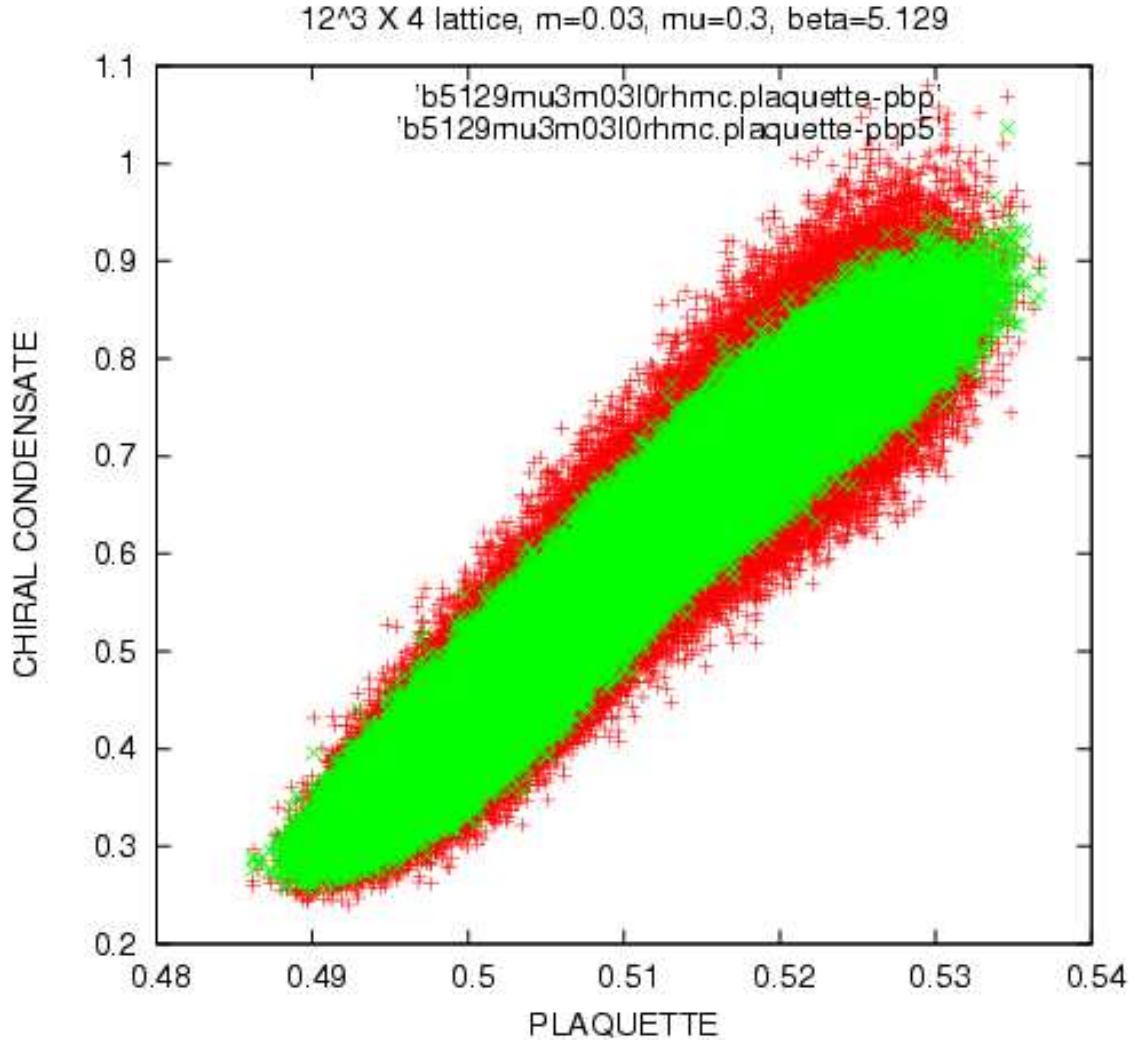


Figure 8: $\bar{\psi}\psi$ versus S_g for each configuration on a $12^3 \times 4$ lattice at $m = 0.03$, $\mu_I = 0.3$, $\beta = 5.129$.

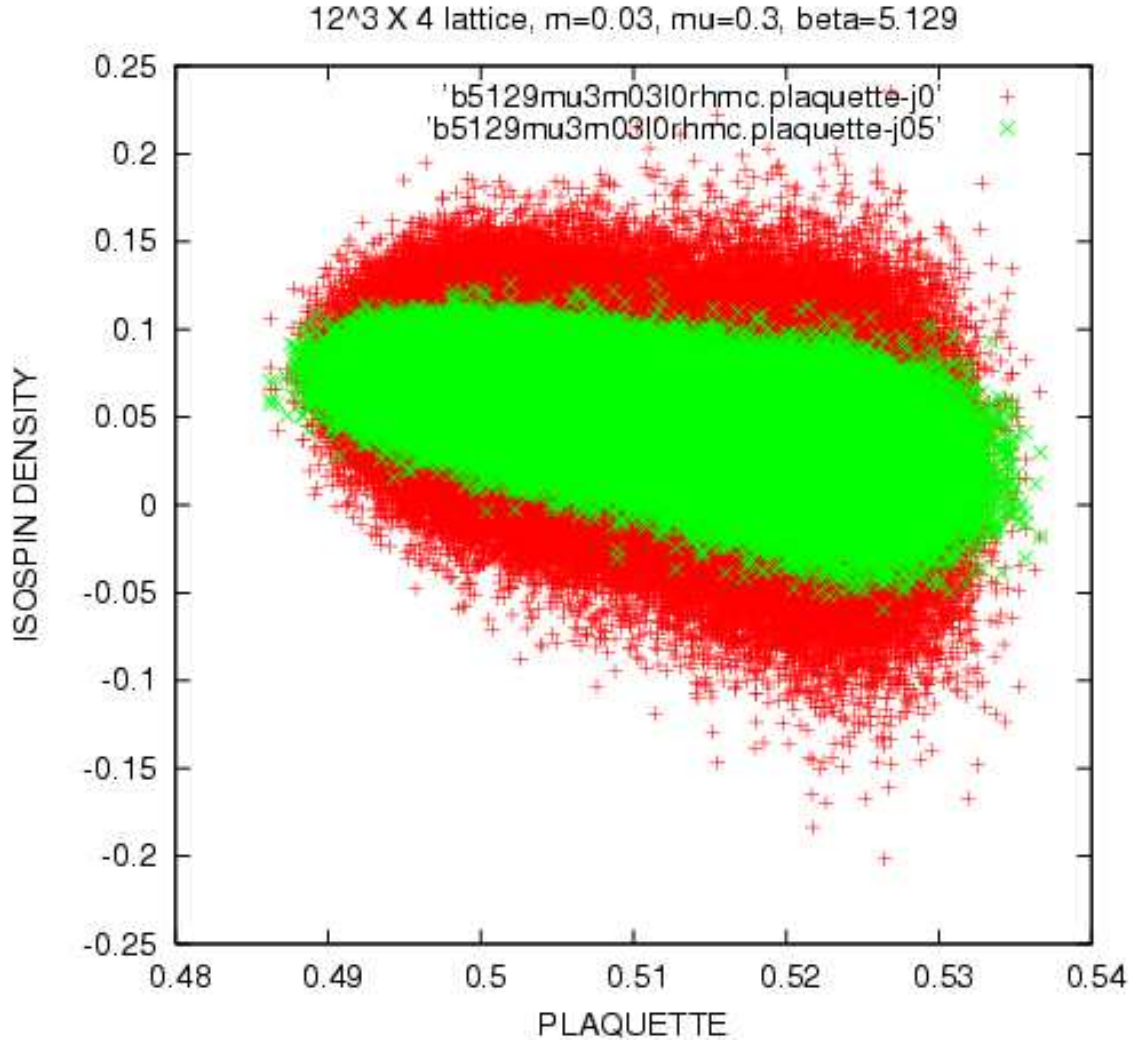


Figure 9: j_0^3 versus S_g for each configuration on a $12^3 \times 4$ lattice at $m = 0.03$, $\mu_I = 0.3$, $\beta = 5.129$.

The chiral susceptibility is defined by

$$\chi_{\bar{\psi}\psi} = \frac{V}{T} \langle \langle \bar{\psi}\psi^2 \rangle - \langle \bar{\psi}\psi \rangle^2 \rangle \quad (2)$$

where the $\bar{\psi}\psi$ s on the right-hand side are lattice averaged quantities.

Finite size scaling *at* the critical point yields

$$\chi_{\bar{\psi}\psi}(L, T_c) = L^{\frac{\gamma}{\nu}} \tilde{\chi} \quad (3)$$

This means that if we plot $L^{-\frac{\gamma}{\nu}} \chi_{\bar{\psi}\psi}(L, T_c)$ as functions of m for different L s, the curves should intersect at the critical point. The graphs of this quantity for $L = 8$ and $L = 12$ for each μ_I , do indicate that the curves cross somewhere between $m = 0.025$ and $m = 0.03$ consistent with our estimates of the positions of the critical points from the Binder cumulants. We take $\gamma = 1.237$ and $\nu = 0.630$ as the 3-D Ising model critical indices.

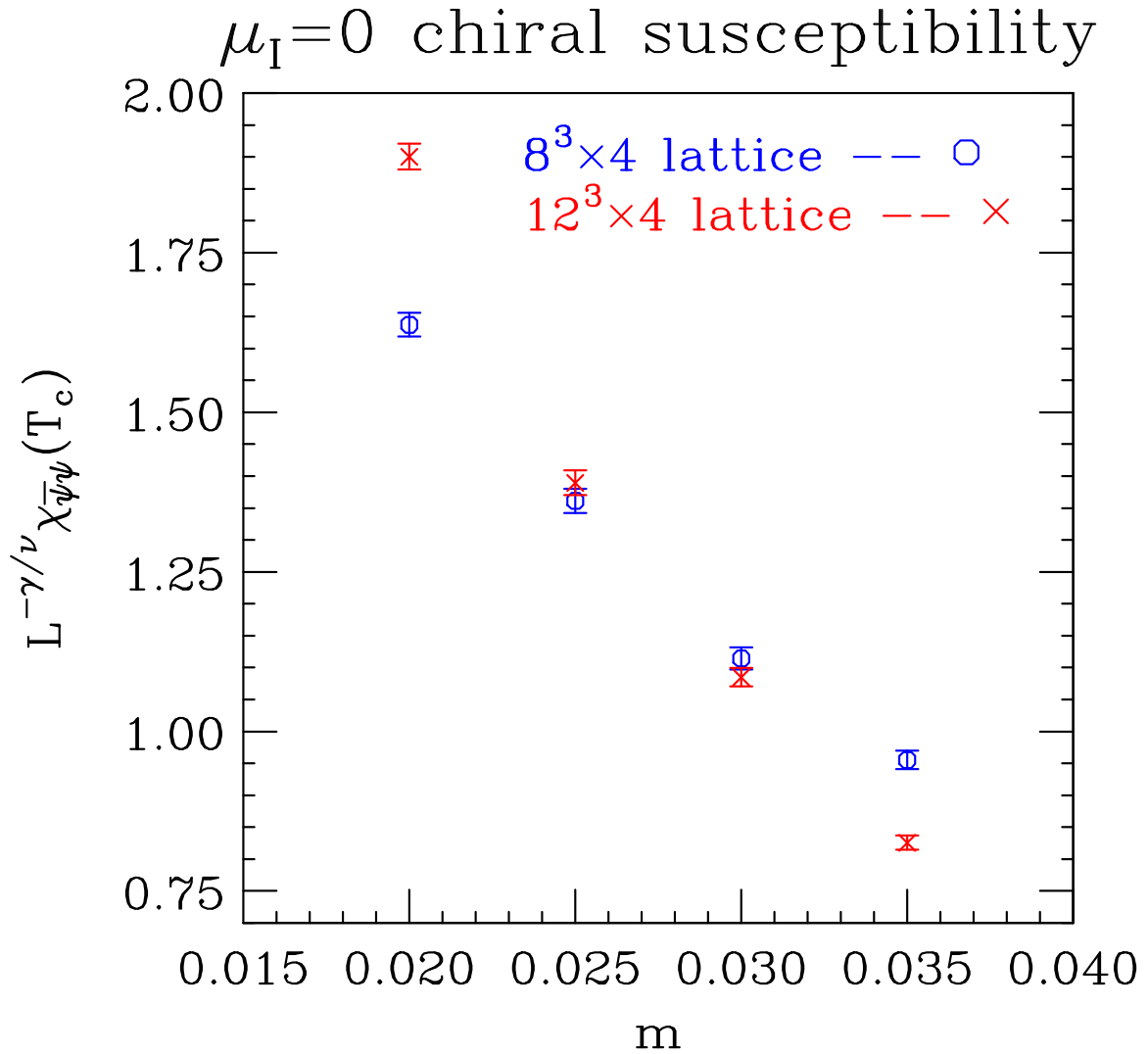


Figure 10: Finite size scaling for the peak of the chiral susceptibilities at $\mu_I = 0$

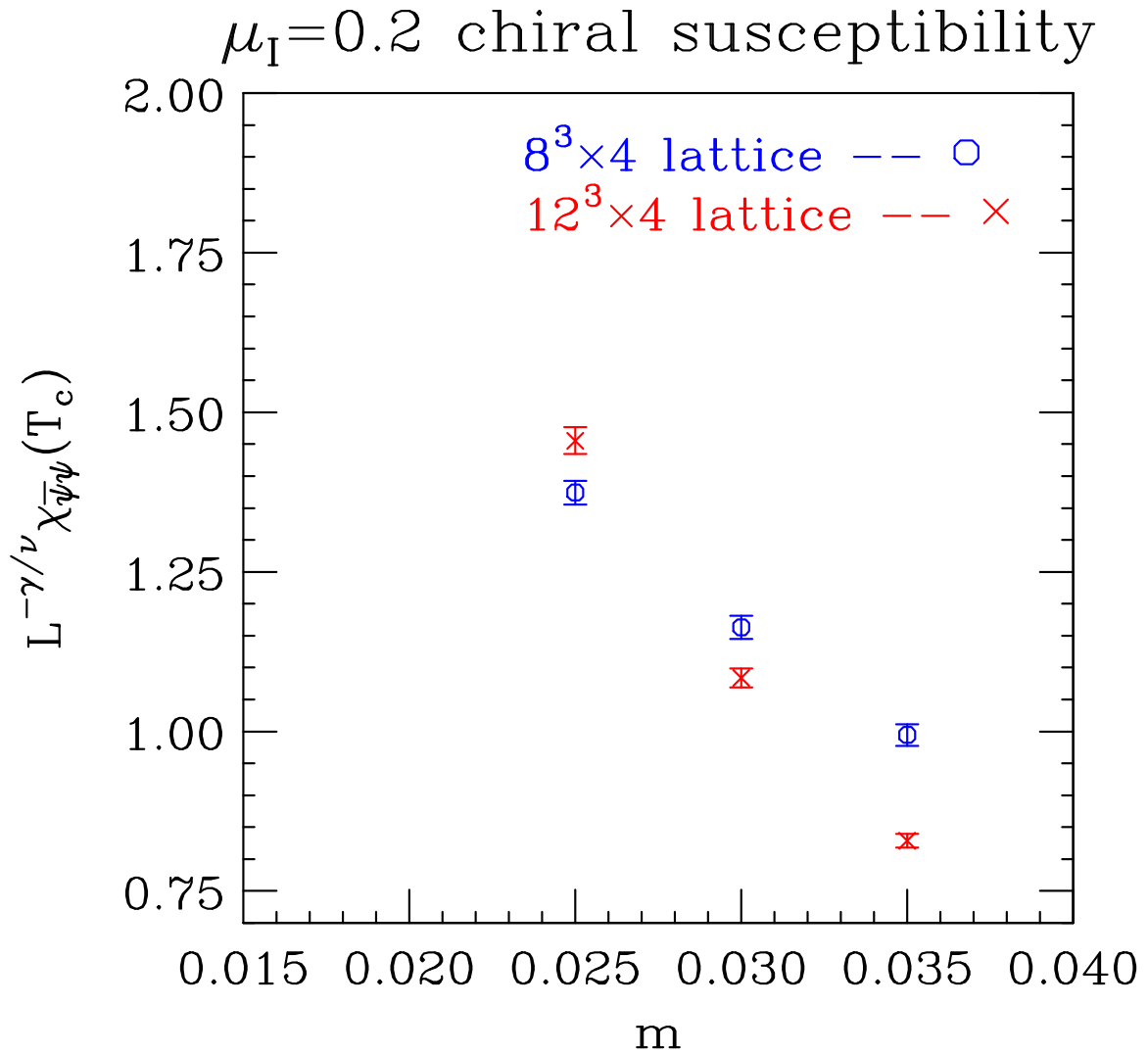


Figure 11: Finite size scaling for the peak of the chiral susceptibilities at $\mu_I = 0.2$

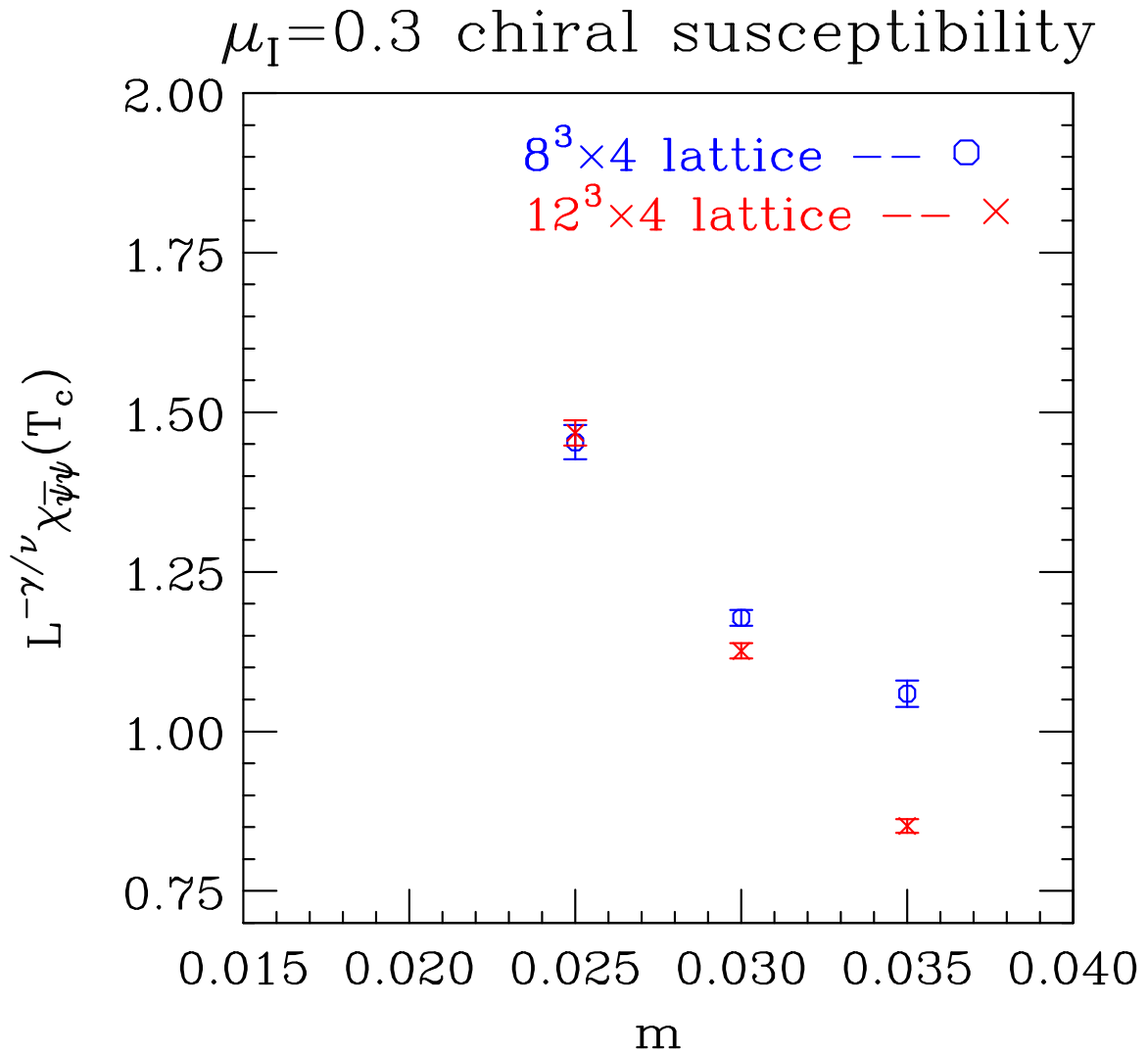


Figure 12: Finite size scaling for the peak of the chiral susceptibilities at $\mu_I = 0.3$

Equation-of-State

The equation-of-state (EOS) expresses the pressure p , the entropy density s and the energy density ϵ as functions of temperature T and μ_I . The pressure p is simply related to the partition function through:

$$p = \frac{T}{V} \ln Z(T, \mu_I). \quad (4)$$

However, we do not actually measure the partition function Z in our simulations, only observables. $Z(T, 0)$ can be calculated by numerically integrating

$$\frac{d \ln Z}{d\beta} = \left\langle 6 \frac{V}{T} S_g \right\rangle \quad (5)$$

We can then numerically integrate

$$\frac{d \ln Z}{d\mu_I} = \left\langle \frac{N_f V}{8 T} j_0^3 \right\rangle \quad (6)$$

at constant β , where I_3 is the the isospin of the

configuration, to obtain $Z(T, \mu_I)$.

To obtain T in physical units requires knowledge of the running of the coupling constant ($\beta = \beta(a)$). This is determined at $\mu_I = 0$.

Once this running of the coupling constant is known, this can be used to determine ϵ , since

$$\epsilon = \frac{T^2}{V} \frac{\partial}{\partial T} \ln Z \quad (7)$$

We are currently performing simulations on $12^3 \times 4$ lattices at $m = 0.03$. At each of a chosen set of β values we perform simulations at sufficient values of μ_I , to enable us to determine the EOS outside of the superfluid region.

The necessary zero-temperature subtractions will be made using simulations on $12^3 \times 24$ lattices at the same β s used at finite temperature, and $\mu_I = 0$.

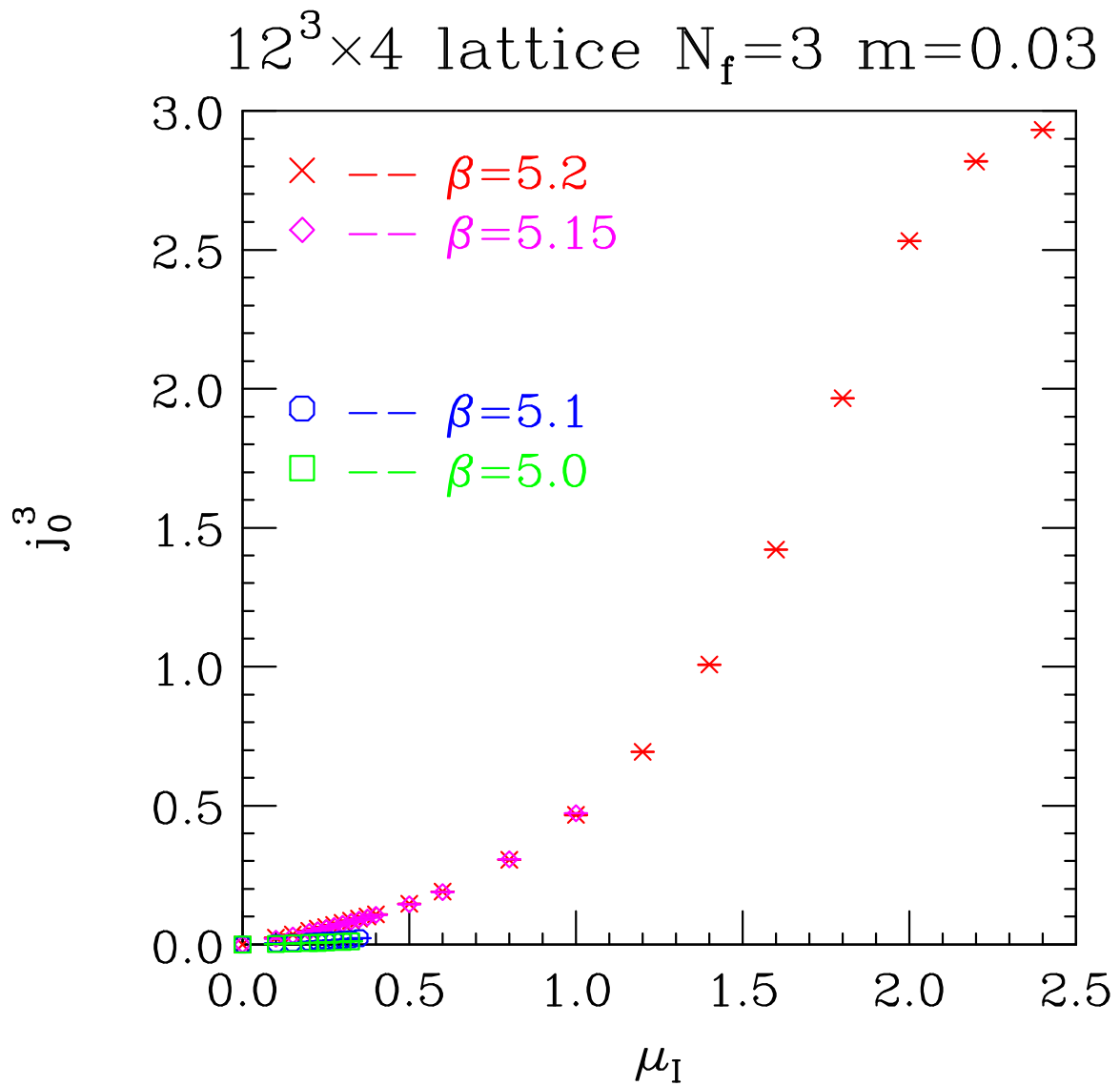


Figure 13: Isospin density as functions of μ_I at fixed β values

$12^3 \times 4$ lattice $N_f=3$ $m=0.03$

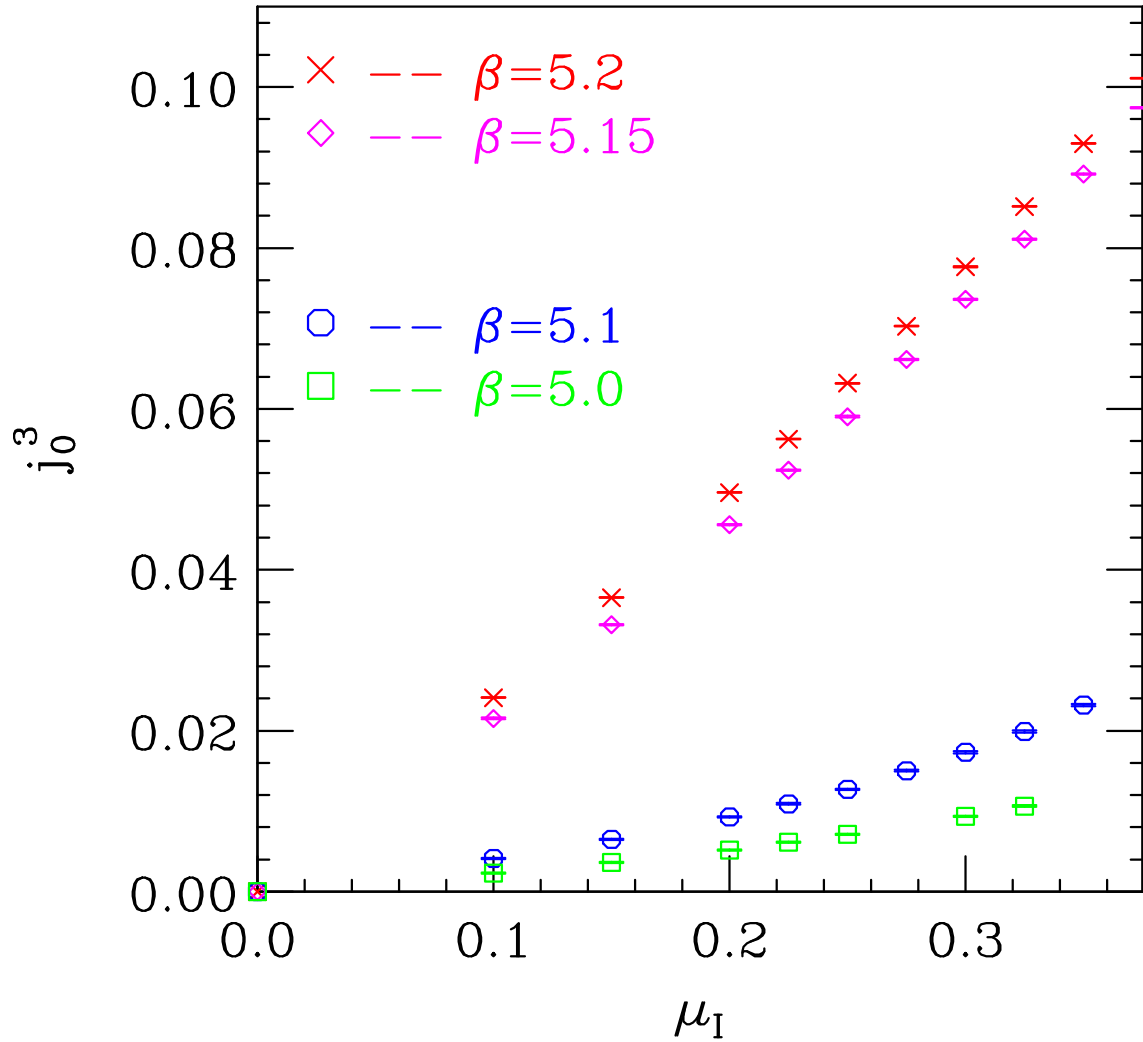


Figure 14: Isospin density as functions of μ_I at fixed β values

Discussion and conclusions

- The phase-quenched approximation to lattice QCD at small chemical potential $\mu < m_\pi/2$, appears to preserve the phase structure.
- There does not appear to be a critical endpoint in this region. This agrees with analytic continuation methods (de Forcrand and Philipsen). The critical mass $m_c(\mu_I)$ in lattice units appears to be almost independent of μ_I . This means that it will decrease in physical units.
- Does increasing μ_I soften the finite temperature transition simply because it reduces the chiral flavour symmetry?
- Better determination of the order parameter (magnetization) is needed. The fact that the Binder cumulants of the chiral condensate for different lattice sizes intersect very close to the Ising value

appears to justify using the chiral condensate instead of the order parameter.

- Using the exact RHMC algorithm is essential for reliable predictions.
- The Fodor and Katz determination of the critical endpoint from reweighting is $T_E = 162(2)$ MeV and $\mu = 120(13)$ MeV. Since $\mu > m_\pi/2$ this is beyond the reach of both phase-quenched and analytic-continuation methods.
- The phase quenched approximation appears to be a good starting point for reweighting. Need better methods of approximating the fermion determinant (or at least its phase).
- We are performing simulations along lines of constant β to determine the equation-of-state for phase-quenched QCD to compare with that for full QCD. At low β s we are restricted to $\mu_I <$

m_π . At high β s where the system is in the plasma phase for all μ_I s, we can cover the whole range of μ_I . What can we learn from the resonance gas model and χ PT?

- Our χ QCD action at finite μ in the phase-quenched approximation would appear to be a better starting point than the conventional action.
- Clearly better methods are needed for QCD at finite baryon-/quark-number density.

These simulations are performed on Tungsten and Copper at NCSA, Bassi and Jacquard at NERSC, DataStar at SDSC/NPACI, and Jazz and Linux PCs at Argonne.